VOL. 10, NO 20, NOVEMBER, 2015 ISSN 1819-6608
ARPN Journal of Engineering and Applied Sciences

www.arpnjournals.com

TRANSONIC FLOW PAST SYMMETRICAL UNSWEPT AND SWEPT WINGS WITH ELLIPTIC NOSE

A. N. Ryabinin
Saint-Petersburg State University, University Emb, St. Petersburg, Russia
E-Mail: a.ryabinin@spbu.ru

ABSTRACT

The spatial flow around a wing with symmetrical airfoil is studied. Solutions of Reynolds-averaged Navier-Stokes equations are obtained with Ansys CFX - 13 finite volume solver. A three-dimensional mesh with elongated along the wingspan elements near the wing is used. The dimensions of supersonic regions reduce at the wing tip. Flow past a wing is accompanied by periodic oscillations of lift force. The coalescence of two supersonic regions is detected near the wing tip for swept tapered wings or near wing root for unswept untapered wing. At Mach number that corresponds to coalescence of supersonic regions the average lift is not equal to zero.

Keywords: transonic flight, supersonic regions, lift oscillations, swept wing.

INTRODUCTION

Numerical studies demonstrated that the transonic flow around an airfoil with surface of small curvature is sensitive to the changes in the parameters of the free flow [1]. Sensitivity is caused by the interaction of local supersonic regions near the airfoil. Two supersonic regions are formed above the area of small curvature. The increase in the Mach number or the increase in the angle of attack leads to arising and expansion of supersonic regions and rapprochement. At the moment of coalescence of two regions the pressure distribution and the lift force abruptly change. This phenomenon was studied for 2D flows in details. It takes place for a number of symmetrical airfoils [1, 2, 3], and for an asymmetrical airfoil J-78 whose upper surface is nearly flat in the midchord region [1, 2, 3]. Instability of supersonic regions was studied for asymmetric airfoils Drela Apex 16 and Boeing 737 Outboard [4, 5, 6, 7]. Flow past airfoil Witcomb with the aileron was studied in [5, 6, 7]. In [8] DSMA532b with the aileron was examined. Aileron deflection leads to a flattening of the airfoil profile near the aileron-airfoil juncture or even to the formation of cavity.

In the 3D case, this type of instability is poorly studied. Flow past the wing is not a real 2D. Airfoil varies along its span. Typically, the wing has a twist. At the root of the wing the angle of attack is greater than the angle of attack at the wing tip. Recently we studied the case of spatial flow past wing segment J-78 with a twist [9, 10]. In [11] 3D flow past unswept wing with elliptic nose was studied. In this paper, the study of 3D flow past swept and unswept wings with elliptic nose is presented.

WING DESCRIPTION

We consider a three-dimensional flow past a smooth wing with symmetric airfoil of thickness h whose midpart is a couple of segments parallel to the x axis. The nose is an elliptic arc [3]. The length of the nose portion of the airfoil is equal to 0.3 chord c. Two circular arcs of radius $R = b + h/2$ constitute the tail of the same length as the nose, where b is the distance from the circumcenter to the x axis:

$$\begin{aligned} y(x) &= \pm\frac{h}{2}\sqrt{\left(2-\frac{x}{0.3}\right)\frac{x}{0.3}} \quad \text{if} \quad 0 \le x \le 0.3, \\ y(x) &= \pm\frac{h}{2} \quad \text{if} \quad 0.3 \le x \le 0.7, \\ y(x) &= \mp b \pm \sqrt{b^2 + 0.3^2 - (x-0.7)^2} \quad \text{if} \quad 0 \le x \le 1, \end{aligned} \tag{1}$$

where x and y are the Cartesian coordinates, divided by the airfoil chord c. The chord of unswept untapered wing is 1 m; the span of unwept wing is 4 m or 3 m. The root chord of the swept wing c_r is equal to 1 m; the tip chord c_t is equal to 0.5 m. So the taper ratio c_t / c_r = 0.5, mean aerodynamic chord c_{MAC} = 0.75 m. Airfoil thickness h = 9 %. The wingspan is equal to 4 m. The quarter chord sweep angle $\Lambda_{0.25}$ = 15 degrees.

GENERATION OF 3D MESH

In the numerical simulation of 3D streams of gas or fluid one of the most important tasks is to reduce the size (number of elements) of computational mesh. Size reduction saves computing resources and reduce the calculation time. Opportunity to reduce the mesh size exists for flows in which the flow parameters vary along a certain direction weaker than in other ones. The increasing of the size of the elements of the computational mesh along this direction reduces the number of cells. Such a technique is used, for example in the boundary layer simulation, wherein the gas velocity increases sharply with arising of distance from the surface, while along the surface velocity varies considerably weaker. Another case

of practical importance is the transversal flow around elongated body, such as an airplane wing. Flow parameters variation along the wing is much less, than across, so the use of the elementary cells, extending along the wingspan, significantly reduces the size of the computational mesh. Meshing with elongated across the flow elements applied to the calculation of the flow around the wing was developed in [12, 13].

2D hybrid mesh was generated using the package Gmsh [14]. Sketch of 2D mesh is presented in Figure-1.

The outer boundary of the 2D lens-type computational domain is composed by two curves Γ_1 and Γ_2. The size of domain along the x axis is 80 chords; the size of domain along the y axis is 200 chords. A program written in Pascal language transformed it into a three-dimensional mesh. The mesh is in the TGrid / Fluent format [15], which is suitable for the calculation in the package Ansys CFX [16]. In this paper we used a method [13] for generating a three-dimensional mesh with elements elongated along a wing. The basis of generating is the two-dimensional mesh. Elementary volumes have hexahedral shape near the surface of the wing in the boundary layer and the pentahedral shape in the rest part of the mesh. Grid is constructed sequentially by parallel transport of a two-dimensional mesh along the wing and the mesh scaling. Computational domain includes the region that surrounds the wing tip. Total size of computational domain along wingspan is 14.5 root chords for the swept wing. The sizes of domain along wingspan for unswept wings are 13.5 and 14.5 chords for aspect ratios 3 and 4 respectively.

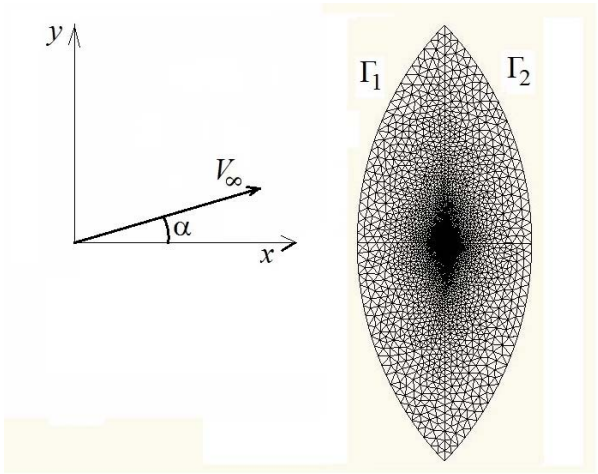

Figure-1. Sketch of 2D mesh.

Most of the calculations are performed with 30 layers in the transverse direction along the wing. The total number of elements in this case is equal to 1,435,836. However, a few calculations are carried out with 50 layers (2, 104, 676 elements). Calculations demonstrated the independence of the results on mesh size.

NUMERICAL METHOD

On the inflow boundary the direction (angle of attack α), temperature T_∞ and the Mach number M_∞ of the free-stream flow are set. On the outflow boundary the average static pressure p_∞ is given. The no-slip condition and vanishing flux of heat are used on the wing surface. Specific heat of air at constant pressure is equal to 1004.4 J / (kg K). Molar mass is equal to 28.96 kg/kmol. We use the Sutherland formula for molecular viscosity. The turbulence level is set to 1%.

Solutions of Reynolds-averaged Navier-Stokes equations are obtained with Ansys CFX - 13 finite volume solver [16] based on high-resolution discretization scheme [17]. Implicit second-order accurate backward Euler scheme is used to solve for time steps. The non-dimensional thickness of the first mesh layer y^+ is approximately equal to 1. The standard model of turbulence k-ω SST [18] is used.

The angle of attack α is equal to zero, the pressure p_∞ is 26434 Pa, temperature T_∞ is equal to 223.15 K. Thus, the parameters of the incident flow match the standard atmosphere at an altitude of 10 km, and the Reynolds number Re is equal to $7.1 \cdot 10^6$.

RESULTS OF CALCULATIONS

Calculations show that in the case of unswept untapered wing the dimension of supersonic region reduces at the wing tip. Figure-2 illustrates a situation when above the wing there are two supersonic regions. If aspect ratio of the wing is 4 and $M_\infty \le 0.86$ there are two supersonic regions both above and under the wing.

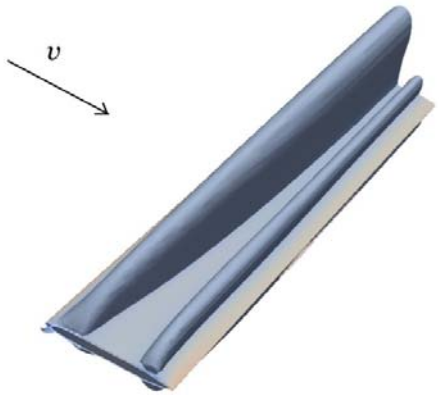

Figure-2. Supersonic regions around the unswept wing. Aspect ratio is equal to 4. Free stream Mach number $M_\infty = 0.8605$.

With increasing Mach number of the incident flow, these regions merge at the wing root. Flow becomes asymmetrical. For example at $M_\infty = 0.8605$ asymmetrical flow at the wing root is shown in the Figure-3. There are separated supersonic regions above the wing and single region under the wing.

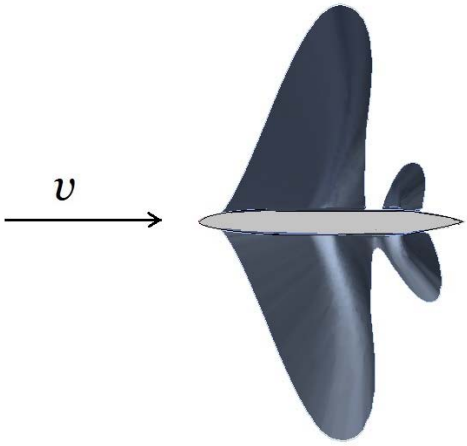

Figure-3. Supersonic regions at the root of unswept wing. Aspect ratio is equal to 4. Free stream Mach number $M_\infty = 0.8605$.

Free stream Mach number M_∞ at which coalescence occurs depends on wing aspect ratio. If aspect ratio is 4 then coalescence exists at $M_\infty > 0.86$. If aspect ratio is 3 then coalescence exists at $M_\infty > 0.864$. The average value of the lift coefficient is not zero in the asymmetric mode. The average values of lift coefficient of the unswepted wings with two separated supersonic regions near both wing sides are 0.0037 and 0.0074 for aspect ratios 3 and 4 respectively.

Coalescence of supersonic regions above and under swept tapered wing occurs near the wing tip. Figure-4 demonstrates the configuration of supersonic regions at $M_\infty = 0.8605$. The narrowest gap between two supersonic regions is situated at a distance of 0.7 m from the wing tip. Increasing of M_∞ leads to merging of these regions at this place. Figure-5 presents supersonic regions at $M_\infty = 0.89$. One can see two separated regions near the root and near the tip of wing.

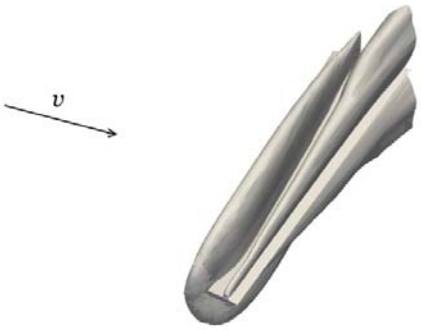

Figure-4. Supersonic regions around the swept wing. Free stream Mach number $M_\infty = 0.882$.

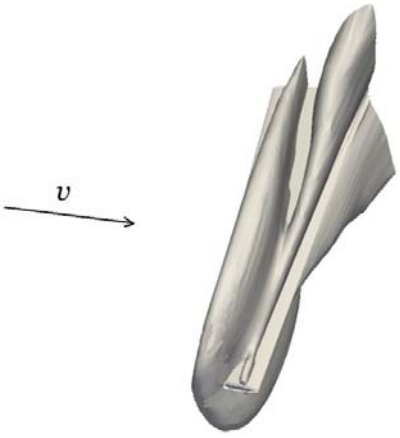

Figure-5. Supersonic regions around the swept wing. Free stream Mach number $M_\infty = 0.89$.

The solutions show self-sustained oscillations (buffet) due to separation of the boundary layers from the upper and lower surfaces of the wing in the aft region. It leads to periodic oscillations in the lift. The same phenomenon was observed in 2D case [3]. As an example, Figure-6 shows the lift coefficient of the wing as a function of time.

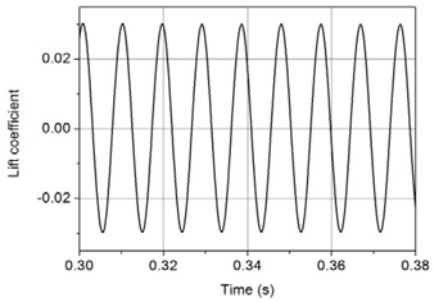

Figure-6. Oscillation of lift force coefficient of the swept wing at $M_\infty = 0.86$.

Amplitude of the oscillations depends on free-stream Mach number. If coalescence of supersonic regions occurs, oscillations do not exist. Figure-7 demonstrates dependence of lift force coefficient on M_∞ for swept wing.

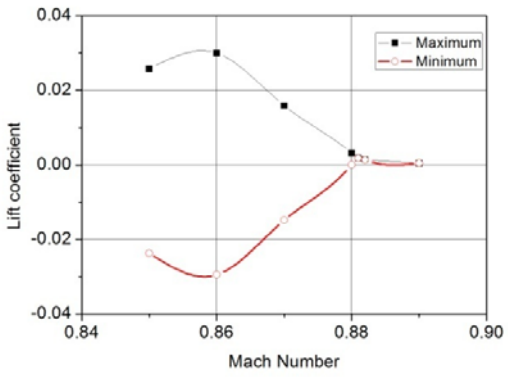

Figure-7. Lift force coefficient of the swept as a function of Mach number M_∞.

Figure-8 illustrates the Strouhal number $St = fc_{MAC}/V_\infty$ as a function of Mach number M_∞.

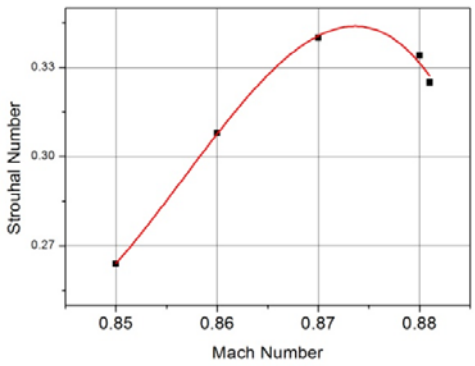

Figure-8. Strouhal number of lift oscillation as a function of free stream Mach number.

Strouhal numbers of lift oscillations of unswept wings close to ones of swept wing.

CONCLUSIONS

The calculations of three-dimensional transonic flow past symmetrical swept and unswept wings revealed features of the flow in the certain range of free stream Mach numbers. This range corresponds to coalescence of the supersonic regions above the upper surface and under lower surfaces of the wing. The dimensions of supersonic regions reduce at the wing tip. Flow past a wing is accompanied by periodic oscillations of lift force if supersonic regions are splitted. The coalescence of two supersonic regions is detected at the wing root for unswept untapered wings or not far from the tip of swept tapered wing. At Mach number that corresponds to coalescence, the average lift is not equal to zero.

ACKNOWLEDGEMENT

This work was supported by RFBR (grant 13-08-00288). Studies were performed using computing resources of Resource Center "Computing center of St. Petersburg State University" (http://cc.spbu.ru).

REFERENCES

[1] Kuzmin A. 2012. Non-unique transonic flows over airfoils. Computers and Fluids. 63: 1-8.

[2] Jameson A. *et al*. 2012. Futher studies of airfoils supporting non-unique solutions in transonic flow AIAA Journal. 50(12): 2865-2881.

[3] Kuz'min A. 2010. Bifurcations of transonic flow past simple airfoils with elliptic and wedge-shaped noses. J. Applied Mechanics and Technical Physics. 51(1): 16-21.

[4] Kuz'min A. 2009. Bifurcation and buffet of transonic flow past flattened surfaces. Computers and Fluids. 38: 1369: 1374.

[5] Kuzmin A. G. and Ryabinin A. N. 2013. Whitcomb airfoil anomalous behavior of lift coefficient in transonic flight (in Russian). In Aerodynamics, R. N. Miroshin, Editor. St. Petersburg. pp. 125-130.

[6] Kuzmin A., Ryabinin A. 2012. Airfoils admitting anomalous behavior of lift coefficient in descending transonic flight. The Seventh International Conference on Computational Fluid Dynamics, Big Island, Hawaii. URL:

http://www.iccfd.org/iccfd7/assets/pdf/papers/ICCFD7-4301_paper.pdf.

[7] Kuzmin A. and Ryabinin A. 2014. Transonic airfoils admitting anomalous behavior of lift coefficient. Aeronautical Journal. 118(1202): 425-433.

[8] Ryabinin A. N. 2014. Influence of aileron position on transonic flow past an airfoil (in Russian). Vestnik Sankt-Peterburgskogo Universiteta. Matematika, mekhanika, astronomia. 1(2): 303-310.

[9] Ryabinin A. 2015. Calculation of transonic flow past the twisted wings. Mechanics - Seventh Polyakhov's Reading, 2015 International Conference on. pp. 1-5.

[10] Ryabinin A. N. 2015. Numerical study of transonic flow past twisted wing J-78 (in Russian). Vestnik Sankt-Peterburgskogo Universiteta. Matematika, mekhanika, astronomia. 2(2): 257-265.

[11] Ryabinin A.N. 2014. Calculation of spatial transonic flow past a wing with symmetrical airfoil (in Russian). Estestvennye I matematicheskie nauki v sovremennom mire. 25: 80-84.

[12] Bogatyrev V. V. 2012. An algorithm for generating swept volume meshes near an aircraft wing. TsAGI Science Journal. 43(1): 87-100.

[13] Ryabinin, A.N., 2014, Generation of 3D meshes near the twisted wing for calculation of transonic flow (in Russian). Estestvennye i matematicheskie nauki v sovremennom mire. 23: 41-45.

[14] Geuzaine Ch., Remacle J.-F. 2014. Gmsh Reference Manual, 278 p. URL: http://geuz.org/gmsh/doc/texinfo/gmsh.pdf.

[15] TGrid 5.0 User's Guide. 2008. Lebanon: ANSYS, Inc., 281 p. URL: https://www.sharcnet.ca/Software/TGrid/pdf/ug/tgrid50-ug.pdf.

[16] ANSYS CFX-Solver Modeling Guide. Release 13.0, 2010, Canonsburg: ANSYS, Inc. p. 604.

[17] Barth T. J. and Jespersen, D. C. 1989. The design and application of upwind schemes on unstructured meshes. AIAA Paper. 89-0366: 1-12.

[18] Menter F. R. 2009. Review of the shear-stress transport turbulence model experience from an industrial perspective. Int. J. of Computational Fluid Dynamics. 23(4): 305-316.